European Journal of Pharmaceutical Sciences 37 (2009) 563–572

Contents lists available at ScienceDirect

European Journal of Pharmaceutical Sciences

journal homepage: www.elsevier.com/locate/ejps

Design and influence of γ-irradiation on the biopharmaceutical properties of nanoparticles containing an antigenic complex from *Brucella ovis*

Raquel Da Costa Martins[a], Carlos Gamazo[b], Juan Manuel Irache[a,*]

[a] Department of Pharmacy and Pharmaceutical Technology, University of Navarra, C/Irunlarrea 1, 31008 Pamplona, Spain
[b] Department of Microbiology and Parasitology, University of Navarra, C/Irunlarrea 1, 31008 Pamplona, Spain

ARTICLE INFO

Article history:
Received 25 February 2009
Received in revised form 3 April 2009
Accepted 3 May 2009
Available online 12 May 2009

Keywords:
Brucellosis
Nanoparticles
Vaccine
γ-Irradiation
Sterilization

ABSTRACT

Despite vaccination campaigns, brucellosis is still one of the most common bacterial zoonosis in the world. This work describes the development of a novel formulation strategy to the delivery of the *Brucella ovis* antigenic extract (HS) into ovine mucosal surfaces. Thus, HS was entrapped in conventional and mannosylated poly(anhydride) nanoparticles by the solvent displacement method, and the resulting nanosystems were γ-irradiated to accomplish the sterilization required for the ophthalmic administration route. Sterilization, at either 10 kGy or 25 kGy, did not modify the size, morphology and antigen content of the nanoparticles. Similarly, the integrity and antigenicity of the entrapped antigen were not affected by γ-irradiation. The 25 kGy γ-irradiation dose seemed to influence negatively the HS release from the carriers. However, and in accordance with the Pearson's correlation, all the release patterns followed a similar tendency. Furthermore, the stability of the vaccine systems on lachrymal and nasal ovine fluids, showed that γ-irradiation had no significant effects on the vaccine systems. Since all the vaccine systems accomplished the pharmacopoeial biological tests required for γ-irradiation doses under 25 kGy, these results are highly suggestive for the use of HS loaded poly(anhydride) nanoparticles as an efficient vaccine delivery system for brucellosis immunoprophylaxis, especially for ophthalmic administration.

1. Introduction

Brucellosis is one of the major contagious bacterial zoonosis worldwide (Boschiroli et al., 2001) and some *Brucella* spp. has being considered as biological warfare agents (level B, classification by the United States Centers for Disease Control) (Greenfield et al., 2002). *Brucella* spp. may affect sheep, goats, rams, cattle, swine, dogs, rodents and several other animals (Cutler et al., 2005; Whatmore et al., 2008). Humans become infected by coming in contact with animals or contaminated animal products causing a range of long-lasting or chronic symptoms (Young, 1995).

Ovine brucellosis is an infectious disease caused by both *Brucella ovis* and *Brucella melitensis*, and it causes important losses in ovine industry (abortion, infertility and mortality). Taking in account that the human disease demands complex and protracted treatment schedules that still are not always effective, and that the global dissemination of animal brucellosis is not achieved, eradication of this zoonosis will only be feasible with an adequate animal vaccine.

Nowadays, the live attenuated vaccine *B. melitensis* Rev1 is the most effective immunoprophylactic system available against ovine brucellosis, which involves either subcutaneous or ocular administration routes (Blasco, 1997). Nevertheless, among all the drawbacks of the attenuated strains, Rev1 displays high residual virulence for both animals and humans, produce abortions, infertility, and it is resistant to streptomycin (Blasco, 1997; Blasco and Diaz, 1993). Another inconvenience in the use of this vaccine is the long persistence in the immunized animal, due to the high level persistence of circulating antibodies (against the smooth lipopolysaccharide), which interfere with serological diagnosis, avoiding the differentiation between the infected animals and the vaccinated ones (Schurig et al., 2002). Other disadvantage of Rev1 is that its use is not allowed in countries officially free from *B. melitensis* such as Canada and USA, most of Northern Europe, Australia and New Zealand. Recently, another commercial vaccine available against ovine brucellosis has been proposed (Schurig et al., 1991). This vaccine is based on the live attenuated *Brucella abortus* RB51, however, although does not interfere with the serological diagnosis, it has been proven to be not so effective against *B. ovis* in rams as Rev1, being neither able to protect nor reduce the severity of the infection or the development of genital lesions (Jimenez de Bagues et al., 1995). In addition, RB51 also offers a number of drawbacks including rifampicin resistance and lack of effectiveness when prevalence is high (Moriyon et al., 2004).

* Corresponding author. Tel.: +34 948 425600; fax: +34 948 425619.
E-mail address: jmirache@unav.es (J.M. Irache).

0928-0987/$ – see front matter © 2009 Elsevier B.V. All rights reserved.
doi:10.1016/j.ejps.2009.05.002

Subcellular vaccines display important advantages to face the classical live attenuated vaccines handicaps. In this context, the hot saline (HS) subcellular antigenic extract from *B. ovis*, which has been probed to be highly immunogenic (Blasco et al., 1993; Gamazo et al., 1989), is mainly composed by the major membrane antigens like outer membrane proteins (OMPs) and rough lipopolysaccharide (R-LPS). However, due to its non-replicant nature, adequate adjuvants have to be associated to the HS extract, in order to promote cellular mediated immunity, specifically Th1 type (Araya and Winter, 1990; Oliveira and Splitter, 1995). Poly(ε-caprolactone) microparticles containing HS (HS-PEC) were found to be a protective vaccine in mice and ram models (Estevan et al., 2006; Munoz et al., 2006; Murillo et al., 2001). Moreover, the lack of interference in the *B. melitensis* diagnostic tests and the intrinsic avirulence and innocuousness, converted HS-PEC microparticles as an attractive anti-*Brucella* vaccine candidate.

On the other hand, it is well known that the mucosal administration route can mimic the bacteria behaviour and generate immunity at the major portals of pathogen entry. In addition, this type of administration can also be safer with less adverse effects and facilitates its dispensation and application. Regarding the imitation of the *Brucella* infection and colonization patterns, the antigens delivery to mucosal surfaces is of remarkable concern, as it has been shown by the ocular administration of Rev1 vaccine (Blasco, 1997). The need of an adequate adjuvant capable of increase the mucosal immune response and protection without the need of booster doses lead us to purpose the use of poly(anhydride) nanoparticles. These controlled release systems have been proposed as adjuvants since they: (i) protect the loaded antigen from enzymatic degradation, (ii) prolong immune response, (iii) enhance the antigen delivery to the mucosal associated lymphoid tissue (MALT) and (iv) exhibit a strong bioadhesive performance (Almeida and Alpar, 1996; Arbos et al., 2003; Gomez et al., 2007; Motwani et al., 2008). To exploit the potential of these systems, mannosamine was added to the nanoparticles as a specific target ligand. The effectiveness of mannosylated devices in vaccination can be ascribed to their ability to target mannose receptors highly expressed in cells of the immune system [i.e. macrophages and dendritic cells (DCs)], as well as many other lectins with mannose-binding activity (Figdor et al., 2002; Keler et al., 2004; Ramakrishna et al., 2007) triggering the enhancement of the innate immune response (Engering et al., 1997; Jain and Vyas, 2006). These systems can mimic the pathogen entry and exhibit a specific and strong bioadhesive capacity to MALT (Salman et al., 2008), reason why are suitable adjuvants to improve mucosal antigen delivery and to enhance immune response. In fact, several authors have been shown that both antigen loading in nanoparticles and mannosylation of the systems as effective approaches to potentiate immunogenicity, due to the higher antigen uptake and presentation by APCs (Irache et al., 2008).

Therefore, the aim of this work was to design and characterize HS loaded poly(anhydride) nanoparticles intended for mucosal administration, including the ophthalmic one. For this reason we also studied the influence of the γ-irradiation sterilization on the physicochemical properties of the antigenic delivery systems, as well as the *in vitro* stability in both ovine nasal and lachrymal fluids.

2. Materials and methods

2.1. Materials

Gantrez®AN 119 [poly (methylvinylether-co-maleic anhydride)] or poly(anhydride) (MW 200,000) was kindly gifted by International Speciality Products (ISP, Barcelona, Spain). D-Mannosamine hydrochloride, concanavaline A (Con A) and pilocarpine hydrochloride were purchased from Sigma–Aldrich (Barcelona, Spain). BCA™Protein Assay Reagent Kit was from Pierce (Rockford, USA). Acrylamide Criterion™XT Precast gels (18 Comb, 30 μL, 1 mm) and the Silver Stain kit were obtained from Bio-Rad Laboratories (California, USA). Peroxidase-conjugate rabbit anti-sheep immunoglobulin G (heavy and light chain specific) (RaSh H+L) was purchased from Nordic Immunological Laboratories (Tilburg, The Netherlands). PVDF (polyvinylidene fluoride papers, pore size of 0.45 μm) sheets were from Schleicher & Schuell (Germany) and 4-chloro-1-naphtol from Merck (Germany). The rainbow coloured protein molecular weight marker was from Amersham Pharmacia Biotech (Freiburg, Germany). All other chemicals were of analytical grade and supplied from Merck (Madrid, Spain).

2.2. Methods

2.2.1. Extraction and characterization of the HS

The hot saline antigenic complex (HS) was obtained from the strain *B. ovis* REO 198 by the hot saline method described previously (Gamazo et al., 1989). To get a large and homogenous batch of cells for extractions, a thawed vial of stock suspension was streaked onto BAB (Blood Agar Base no. 2, Difco, Detroit, USA) plates, and 24 h cultures were inoculated into a 10 L bioreactor (B. Braun Biotech, Germany), and incubated at 37 °C for 48 h. Live cells were suspended in saline solution (0.85% NaCl, 10 g packed cells per 100 mL), and heated in flowing steam for 15 min. Following centrifugation at 12,000 × *g* for 15 min, the supernatant was dialyzed for 5 days at 4 °C against several changes of deionized water (dH_2O). The dialyzed material was ultracentrifuged for 3 h at 60,000 × *g* and the pellet (HS) washed in dH_2O, freeze-dried and stored at room temperature.

Total protein was determined by the BCA™ Protein Assay method (Smith et al., 1985), with bovine serum albumin as standard. The analysis for 2-keto-3-deoxyoctonate (KDO, exclusive marker of LPS) corrected for 2-deoxyaldoses was performed by the method of Warren modified by Osborn (Osborn, 1963). The batch of antigen used to prepare the vaccine formulation contained 66.4 ± 10.6% protein and 39.5 ± 3.8% rough lipopolysaccharide (R-LPS).

2.2.2. Nanoparticles preparation

Conventional (NP-HS), mannosylated (MAN-NP-HS) and respective control nanoparticles (NP and MAN-NP) were prepared by a modification of the solvent displacement method previously described (Arbos et al., 2002; Salman et al., 2006).

2.2.2.1. Conventional nanoparticles. Four milligrams of the HS antigenic extract were dispersed in 2 mL acetone, under sonication, an added to 100 mg of Gantrez®AN 119 previously dissolved in 3 mL acetone. After 30 min of incubation under magnetic stirring at 300 rpm, the nanoparticles were formed by the addition of an 20 mL ethanol/water mixture (1:1, v/v). Then, the organic solvents were eliminated under reduced pressure (50 mbar, Büchi R-144, Switzerland). The resulting nanoparticles were purified by centrifugal filtration at 3000 × *g* for 20 min (VivaSpin®20 300,000 M.W.C.O., Vivascience, Sartorius group, Hannover, Germany). This step was repeated two times and the filtrates were collected for the quantification of the non-entrapped HS. Finally, nanoparticles were freeze-dried using sucrose (5%) as cryoprotector (Genesis 12EL, Virtis, USA). Control conventional nanoparticles (NP) were prepared in the HS absence.

2.2.2.2. Mannosylated nanoparticles. To obtain mannosylated-coated Gantrez®AN nanoparticles, 100 mg of the poly(anhydride) were dissolved in 5 mL of acetone and incubated overnight with manosammine (1 mg). Then, 4 mg HS was added and sonicated

for 10 min. After 30 min of incubation under magnetic stirring at room temperature, the nanoparticles were formed by the addition of 10 mL of absolute ethanol. Then, the just formed nanoparticles were dispersed in 10 mL of ultrapure water containing 5 mg of mannosamine. The organic solvents were eliminated under reduced pressure (50 mbar, Büchi R-144, Switzerland), and the resulting aqueous nanosuspensions were magnetically stirred for 1 h in order to facilitate the coating of nanoparticles with mannosamine. After incubation, nanoparticles were purified by centrifugation at 3000 × *g* for 20 min (VivaSpin®20 300,000 M.W.C.O., Vivascience, Sartorius group, Hannover, Germany). This step was repeated two times and the filtrates were collected for the quantification of the non-entrapped HS and the non-associated mannosamine. Finally, the suspensions were freeze-dried using sucrose (5%) as cryoprotector (Genesis 12EL, Virtis). Control mannosylated nanoparticles (MAN-NP) were prepared in the HS absence.

2.2.3. γ-Irradiation of Gantrez®AN nanoparticles

Conventional and mannosylated nanoparticles, and respective controls, placed in type 1 glass vials and sealed with a conventional rubber–silicone stopper aluminium crypted, were γ-irradiated at room temperature by using ^{60}Co as irradiation source (Aragogamma, Barcelona, Spain). Doses of 10 kGy and 25 kGy, at a 3.730 kGy/h dose rate, were applied. Then, the correspondent sterility biological tests were performed following the European Pharmacopoeia requirements (European Pharmacopoeia 6th, 2007).

2.2.4. Characterization of the nanoparticles: size, zeta potential, surface morphology and mannosamine content

The particle size and the zeta potential of nanoparticles were determined by photon correlation spectroscopy (PCS) and electrophoretic laser doppler anemometry, respectively, using a Zetamaster analyser system, at 25 °C (Malvern Instruments, Malvern, UK). The diameter of the nanoparticles was determined after dispersion in ultrapure water (1/10) and measured at 25 °C with a dynamic light scattering angle of 90 °C. The zeta potential was determined as follows: 200 μL of the samples were diluted in 2 mL of a 0.1 mM KCl solution adjusted to pH 7.4 (Lambert et al., 2000). The average particle size was expressed as the volume mean diameter (V_{md}) in nanometers (nm), and the average surface charge in millivolts (mV).

Shape and morphology were examined by scanning electron microscopy (Zeiss DSM 940 A, Oberkochen, Germany) with a digital imaging capture system (DISS, Point Electronic GmBh, Halle, Germany). For this purpose freeze-dried formulations were resuspended in ultrapure water and centrifuged at 27,000 × *g* for 20 min at 4 °C. Then, supernatants were rejected and the obtained pellets were mounted on a glass plates adhered with a double-sided adhesive tape onto metal stubs, coated with gold to a thickness of 16 nm (Emitech K550 equipment, United Kingdom).

The yield of the nanoparticles preparation process was determined by gravimetry from freeze-dried nanoparticles as described previously (Arbos et al., 2002).

The amount of mannosamine associated to nanoparticles was estimated by quantification of free mannosamine in the supernatants obtained during the purification step using the O-phthalaldehyde (OPA) fluorimetric assay of primary amines, as described elsewhere (Benson and Hare, 1975).

2.2.5. Antigen loading in the nanoparticles

HS was quantified by the BCA™ Protein Assay method. For control in process purposes (expressed as before freeze-drying in Table 2), HS was estimated from the difference between its initial concentration added and the concentration found in the collected filtrates obtained during the purification step of nanoparticles.

For HS quantification in the final product (expressed as after freeze-drying in Table 2), 10 mg of freeze-dried and γ-irradiated nanoparticles were resuspended in 1 mL of ultrapure water and centrifuged (28,000 × *g*, 20 min, 4 °C). Then, the precipitate was dissolved in 2 mL of acetone/DMF (3:1, v/v) and kept for 1 h at −80 °C. Samples were centrifuged at 28,000 × *g* for 20 min at 4 °C and the pellet was washed with 1 mL acetone and kept 30 min at −80 °C. After centrifugation under the same conditions, pellets were resuspended in 500 μL of ultrapure water to quantify proteins by the BCA™ Protein Assay.

In any case, each sample was assayed in triplicate. HS loading was expressed as the amount of HS (in μg) per mg nanoparticles whereas the entrapment efficiency (EE) was determined by relating the total weight of antigen entrapped in the batch of nanoparticles to the initial weight of antigen and expressed in percentage. For calculations, the following calibration curves were used: (i) a calibration curve of free HS in the filtrates obtained from control conventional nanoparticles ($r^2 > 0.999$), and in the filtrates obtained from control mannosylated nanoparticles ($r^2 > 0.997$), for the control in process purposes and (ii) a calibration curve of free HS obtained after proteins precipitation with acetone/DMF in ultrapure water ($r^2 > 0.999$).

2.2.6. Agglutination assay of mannosylated nanoparticles

The *in vitro* agglutination assay of non-irradiated and γ-irradiated mannosylated nanoparticles using concanavalin A (Con A) was applied to confirm the biological activity of the mannosamine attached to the surface of the nanoparticles. The assays were performed by a modification of a procedure described elsewhere (Salman et al., 2006). Briefly, 50 μL of concanavalin A (1 mg/mL) were added to 200 μL of nanoparticle samples (1 mg/mL) in phosphate buffered saline (PBS, 10 mM, pH 7.4) in the presence of 5 mM calcium chloride and 5 mM magnesium chloride. The turbidity change was monitored in a spectrophotometer at 405 nm in continuous kinetic measurements (Labsystems iEMS Reader MF, Finland).

2.2.7. HS structural integrity and antigenicity

To evaluate the effect of the manufacturing process and γ-irradiation on the HS protein profile and antigenicity, proteins from the freeze-dried nanoparticles were extracted with acetone/DMF (3:1, v/v) as described above, and assayed by SDS-PAGE and immunoblotting. For SDS-PAGE, samples were analysed by using a 12% acrylamide slabs with the discontinuous buffer system of Laemmli and gels stained with Coomassie brilliant blue for proteins. The apparent molecular weight of the proteins was determined by comparing their electrophoretic mobility with that of the molecular mass marker (rainbow coloured protein molecular weight marker, Amersham Pharmacia Biotech, Freiburg, Germany). Immunoblotting was performed with sera from a pool of rabbits experimentally infected with *B. ovis* and with peroxidase-conjugated goat anti-rabbit IgG (Nordic) and 4-chloro-1-naphtol as chromogen as described previously (Gamazo et al., 1989).

2.2.8. In vitro release study

Prior release studies, 5 mg of HS loaded nanoparticles were first resuspended in water and centrifuged (28,000 × *g*, 20 min , 4 °C) in order to avoid sucrose interferences in the assay process. Then, the resulting pellet was dispersed in 500 μL of phosphate buffer (PBS, 10 mM, pH 7.4). Each sample was assayed in triplicate.

The study was conducted at 37 ± 1 °C under horizontal agitation during 30 days in a VorTemp 56™ Shaking Incubator (Labnet International, Inc.). At different time intervals, samples were collected in VivaSpin®2 300,000 M.W.C.O. tubes (Vivascience, Sartorius group,

Hannover, Germany) and centrifuged at 3000 × *g*, for 20 min at 4 °C.

The HS extract was quantified by BCA™ Protein Assay in the collected filtrates (calibration curve of free HS in the filtrates obtained from control conventional nanoparticles, $r^2 > 0.999$, and control mannosylated nanoparticles, $r^2 > 0.997$, in PBS pH 7.4). The structural integrity and antigenicity of the entrapped HS was assessed by SDS-PAGE and immunoblotting, respectively, using the methodology already described. Release profiles were expressed in terms of cumulative release in percentage, and plotted vs. time.

2.2.9. Evaluation of nanoparticles stability in ovine mucosal fluids

The stability of poly(anhydride) nanoparticles was investigated by measuring the turbidity changes as a function of time in different ovine mucosal fluids by spectrophotometry, by modifications of methods described elsewhere (Arbos et al., 2003; Salman et al., 2006). Analysis was performed for mannosylated and conventional nanoparticles and stability was estimated at 2 h post-incubation in the corresponding fluids.

The ovine secretion fluids were obtained in compliance with the regulations of the responsible committee of the University of Navarra in line with the European legislation on animal experiments (86/609/EU). Briefly, 5 mL of an aqueous solution of pilocarpine chlorhydrate (20 mg/mL) was administered subcutaneously to 3 months old Aragonesa male rams (average weight 25 kg, La Protectora, Spain). Then, both lachrymal and nasal fluids were collected by the use of appropriate sterilized poly(ethylene) Pasteur pipets.

For this purpose, conventional and mannosylated nanoparticles loaded with HS from *B. ovis* were resuspended in water (5 mg/mL). Then, each nanosuspension type was added to the corresponding ovine fluid (1:1, v/v). The turbidity changes were monitored in a spectrophotometer at 405 nm in continuous kinetic measurements (Labsystems iEMS Reader MF, Finland) during 2 h (200 μL of sample).

The following equation was applied to calculate the percentage of remaining nanoparticles:

$$\text{remaining NP}(\%) = \left[1 - \frac{\text{Abs}_{t=0} - \text{Abs}_{t=2}}{\text{Abs}_{t=0}}\right] \times 100 \quad (1)$$

in which $\text{Abs}_{t=0}$ and $\text{Abs}_{t=2}$ correspond, respectively, to the initial and 2 h absorbance measured at 405 nm.

2.2.10. Statistical analysis

Data are expressed as the mean ± S.D. of at least three experiments. The Student's *t*-test assessed the nanoparticles characterization. Other statistical significance analysis was processed using the non-parametric Kruskal–Wallis test, followed by Mann–Whitney *U*-test. The Pearson's correlation analysis was applied in order to compare the patterns of the release studies. Statistically significant differences were considered for *p* values of <0.05.

All data processing was performed using the SPSS® statistical software program (SPSS® 16.0.1, Mac OS X, USA).

3. Results

3.1. Characterization of the nanoparticles: size, zeta potential, surface morphology and mannosamine content

Table 1 summarizes the main physicochemical properties of all the designed vaccine formulations.

All freeze-dried formulations displayed homogeneous sizes of around 200–300 nm, with low polydispersion (PDI < 0.2). However, the coating of the nanoparticles with mannosamine significantly increased the mean diameter of the resulting carriers ($p < 0.05$). Concerning zeta potential, conventional and mannosylated nanoparticles displayed negative surface charges, slightly more negative for mannosylated than for control nanoparticles. However, both antigen loaded nanoparticles, NP-HS and MAN-NP-HS, showed similar electronegative surfaces. After sterilization no significant differences in the mean particle size and zeta potential were observed for both mannosylated and conventional nanoparticles.

Similarly, by comparing SEM photographs (see Fig. 1), no evident modifications on the size and morphology of the nanoparticles were visualized after irradiation. All vaccine formulations were found to be homogeneous and spherically shaped.

On the other hand, mannosylation slightly increased the yield of the nanoparticles preparative process. The mannosamine content for mannosylated nanoparticles was found to be close to 30 μg/mg, independently of the HS extract presence.

3.2. Antigen loading in the nanoparticles

Table 2 summarizes the encapsulation efficiency and HS loading in the different formulations tested. For conventional nanoparticles, HS loading was calculated to be about 34 μg HS/mg of nanoparticles, which represented an encapsulation efficiency of about 65%. For mannosylated nanoparticles, in spite of the encapsulation efficiency was about 69%, the HS loading was only 28 μg HS/mg of nanoparticles.

Interestingly, quantification of HS in the filtrates obtained during the purification step (quality control in process analysis) and in the final product, after freeze-drying, gave similar results ($p > 0.05$).

Table 1
Physicochemical characteristics of nanoparticles. NP: conventional nanoparticles; NP-HS: HS loaded conventional nanoparticles; MAN-NP: mannosylated nanoparticles; MAN-NP-HS: HS loaded mannosylated nanoparticles (data expressed as mean ± S.D., $n = 10$).

Vaccine formulation	[a]Size (nm)			Zeta potential (mV)			[b]Yield (%)	[c]Man content (μg/mg NP)
	NO γ-irradiated	10 kGy	25 kGy	NO γ-irradiated	10 kGy	25 kGy		
NP	175 ± 1	175 ± 1	179 ± 2	−28.7 ± 0.7	−29.7 ± 1.6	−29.6 ± 0.8	72 ± 3	–
NP-HS	186 ± 2	185 ± 4	189 ± 4	−37.7 ± 0.7	−38.2 ± 1.4	−36.9 ± 1.8	72 ± 5	–
MAN-NP	272 ± 12*	313 ± 42*	286 ± 21*	−38.2 ± 1.4**	−35.1 ± 1.0**	−38.5 ± 0.8**	81 ± 6	30.2 ± 4.1
MAN-NP-HS	306 ± 11*	335 ± 22*	297 ± 11*	−34.6 ± 1.3	−33.4 ± 1.3	−36.9 ± 1.0	80 ± 5	32.1 ± 4.7

Treatments: NO γ-irradiated: no γ-irradiated nanoparticles; 10 kGy: γ-irradiated nanoparticles at a 10 kGy dose; 25 kGy: γ-irradiated nanoparticles at a 25 kGy dose.

[a] Determination of the nanoparticles volume mean diameter (nm) by photon correlation spectroscopy.

[b] The percentage yield of the polymer transformed into nanoparticles.

[c] Amount of mannosamine coating the nanoparticles.

* $p < 0.05$ for MAN-NP vs. NP, and MAN-NP-HS vs. NP-HS (Student's *t*-test).

** $p < 0.05$ for MAN-NP vs. NP (Student's *t* test).

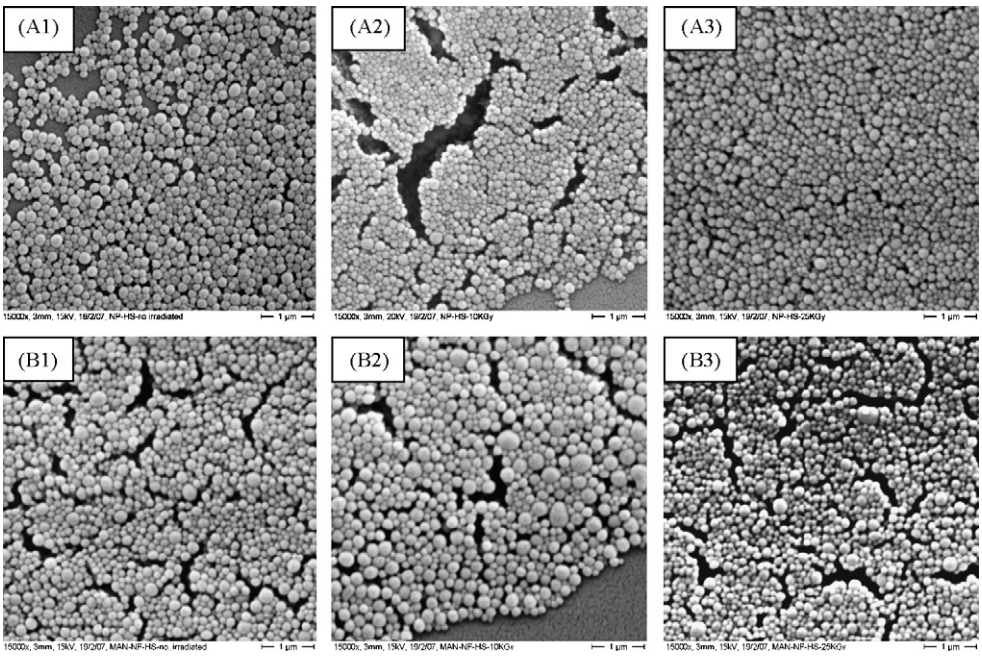

Fig. 1. Surface scanning electronic microfotographs of the different nanoparticles. Lines: (A) NP-HS: HS loaded conventional nanoparticles and (B) MAN-NP-HS: HS loaded mannosylated nanoparticles. Columns: (1) nanoparticles no exposed to γ-irradiation; (2) nanoparticles exposed to a γ-irradiation dose of 10 kGy and (3) nanoparticles exposed to a γ-irradiation dose of 25 kGy.

Table 2
Antigenic content of the vaccine formulations before freeze-drying and after γ-irradiation. NP-HS: HS loaded conventional nanoparticles; MAN-NP-HS: HS loaded mannosylated nanoparticles (data expressed as mean ± S.D., at least $n = 3$).

Vaccine formulation	[a]HS loading (μg/mg NP)				[d]E.E. (%)
	[b]Before f.d.	[c]After f.d.			
		NO γ-irradiated	10 kGy	25 kGy	
NP-HS	34.97 ± 2.34	33.49 ± 0.40	33.97 ± 0.65	33.55 ± 0.94	65 ± 2
MAN-NP-HS	28.28 ± 1.86	27.92 ± 0.20	27.91 ± 0.31	27.61 ± 0.20	69 ± 1

Treatments: NO γ-irradiated: no γ-irradiated nanoparticles; 10 kGy: γ-irradiated nanoparticles at a 10 kGy dose; 25 kGy: γ-irradiated nanoparticles at a 25 kGy dose.
[a] Determination of the protein content by BCA™ Protein Assay.
[b] Before freeze-drying.
[c] After freeze-drying.
[d] Determination of the entrapment efficiency, expressed in percentage, by relating the total weight of antigen entrapped in the batch of nanoparticles to the initial weight of antigen.

3.3. Agglutination assay of mannosylated nanoparticles

In order to confirm the mannose biological activity after mannosylation of poly(anhydride) nanoparticles, an agglutination test was carried out in the presence of the mannose lectin concanavalin A. In this context, non-γ-irradiated mannosylated nanoparticles (MAN-NP) and MAN-NP γ-irradiated at 10 kGy displayed a similar initial lectin binding capacity which was higher than that found for MAN-NP γ-irradiated at 25 kGy (Fig. 2).

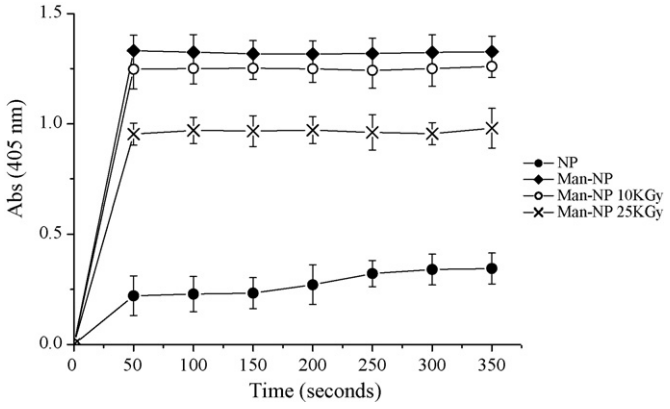

Fig. 2. Con A agglutination assay to confirm the presence of mannose at the surface of the nanoparticles. The turbidity change was reported at 405 nm for 350 s, after the incubation of 200 μL (1 mg/mL) of MAN-NP no γ-irradiated (♦), MAN-NP γ-irradiated at 10 kGy (○), MAN-NP γ-irradiated at 25 kGy (×) and control non-mannosilated NP (●), with 50 μL Con A (1 mg/mL). Data reported as mean ± S.D. ($n = 3$).

3.4. HS structural integrity and antigenicity

Fig. 3 shows the SDS-PAGE and immunoblotting of HS extracted from the γ-irradiated and non-irradiated nanoparticles. As it can be seen, the protein profile of the antigenic complex extracted from the nanoparticles was similar to that of free HS and did not reveal the presence of additional protein bands. Moreover, the extracted HS demonstrated the same reactivity against a pool of sera from experimentally infected rabbits with *B. ovis*.

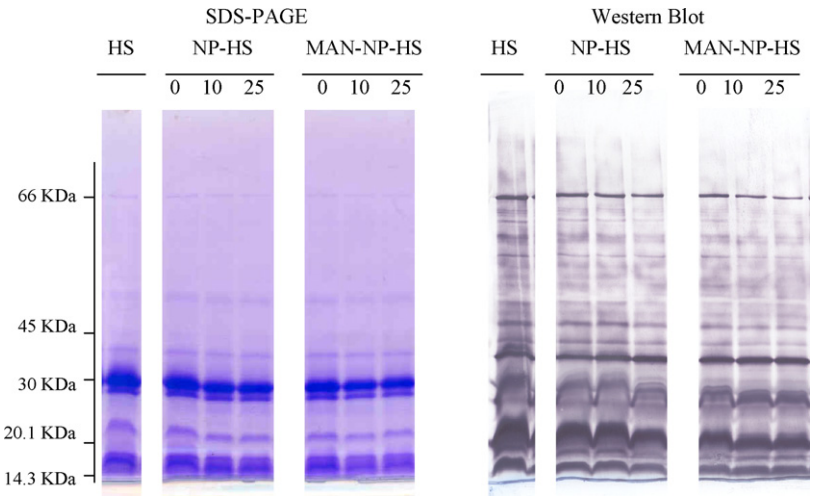

Fig. 3. SDS-PAGE and Coomassie blue stain profiles of free and entrapped HS and Western blot against a pool of sera from *B. ovis* experimentally infected rabbits. Lanes: HS: 40 μg free hot saline antigenic extract; NP-HS: HS loaded conventional nanoparticles; MAN-NP-HS: HS loaded mannosylated nanoparticles. (0) Non-γ-irradiated; (10) γ-irradiation dose of 10 kGy and (25) γ-irradiation dose of 25 kGy.

3.5. *In vitro release study*

Fig. 4 shows the influence of γ-irradiation on the HS release profile from nanoparticles, under physiological conditions (PBS, 10 mM, pH 7.4) for 30 days.

Non-irradiated nanoparticles displayed a biphasic release pattern characterized by a burst effect, followed by a continuous release of the antigen for at least 30 days.

For conventional nanoparticles, the sterilization process appeared to modify the release pattern of HS during the first 24 h ($p < 0.05$). In fact, after this time, about 15% of the loaded antigenic complex was released from control nanoparticles, whereas more than 30% of the loaded HS was released from irradiated particles, irrespective of the γ-ray dose. Nevertheless, after 3 days all the profiles were found similar and, at the end of the experiment, all the formulations had released the same amount of HS.

On the other hand, mannosylation induced a high degree of HS release during the first 24 h. However, in this case, the irradiation of nanoparticles with a 10 kGy dose modified neither the amount of HS released nor the profile of the curve. On the contrary, nanoparticles irradiated with a dose of 25 kGy displayed a burst effect two times higher than for the other two formulations (55% of the loaded HS vs. 25%).

In any case, independently of the type of poly(anhydride) nanoparticle or the irradiation intensity, the Pearson's correlation (Table 3) revealed that all the HS release profiles followed a similar tendency during the 30 days of the experiment.

SDS-PAGE analysis confirmed the stability of formulations within the release, and the average band density of the samples corroborated the kinetic release values obtained (not shown). In addition, the biological activity or antigenicity of the HS, assessed through immunoblotting, was recognized by a pool of sera from experimentally infected rabbits (Fig. 5). Likewise, after 14 days of release, SDS-PAGE and immunoblotting showed that both integrity and the antigenicity of the HS were preserved.

3.6. *Evaluation of nanoparticles stability in ovine mucosal fluids*

To evaluate the *in vitro* stability of poly(anhydride) vaccine formulations in mucosa, the different nanoparticles formulations were incubated in both lachrymal and nasal ovine fluids (Fig. 6). In any case, independently on the medium or γ-dose, all nanoparticle formulations demonstrated high stability for at least 2 h post-incubation, since more than 75% of nanoparticles maintained their integrity and no significant statistical evidences were found between the groups ($p > 0.05$).

In general, both types of nanoparticles (conventional and mannosylated nanoparticles) displayed a slightly higher stability in nasal secretions than in lachrymal fluids. In addition, mannosylation of nanoparticles increased their stability in nasal secretions of about a 6% than for conventional ones.

On the other hand, γ-irradiation did not affect significantly the nanoparticles stability in both ovine biological fluids ($p > 0.05$). Thus, in lachrymal fluids, the higher dose of irradiation (25 kGy) only enhanced the degradation of nanoparticles in about 8%, and in nasal secretions, stability decreased around 5% when compared with non-sterilized carriers.

4. Discussion

Since the delivery of vaccine antigens to mucosal surfaces is of particular interest we have designed conventional and mannosylated poly(anhydride) nanoparticles loaded with the HS antigenic extract for *B. ovis* mucosal immunoprophylaxis. However, when administered by the ophthalmic route, these systems have to accomplish the pharmacopoeial sterility requirements. As the poly(anhydride) polymer is thermo-sensitive, heat sterilization methods, like dry heat and autoclaving, are not appropriate. Radiosterilization is as an effective isothermal process, which allows reaching the required sterility assurance level of 10^{-6}, suitable for the sterilization of thermo-sensitive products, and accepted by the different pharmacopoeias and the European Agency for the Evaluation of Medicinal Products (EMEA). The reference dose of radiosterilization is 25 kGy (minimum absorbed dose), but lower doses may be validated using appropriate sterility tests.

Because each stage of a vaccine development process should result in an improvement of efficacy and safety, we studied the effect of the irradiation on the systems physicochemical characteristics of the carriers and the biological properties of the entrapped antigen.

Firstly, the preparation process of both conventional and mannosylated nanoparticles by the solvent displacement method was optimized to reach an effective HS entrapment. By a simple incubation between the polymer and the antigenic extract, HS loaded conventional nanoparticles were successfully obtained with

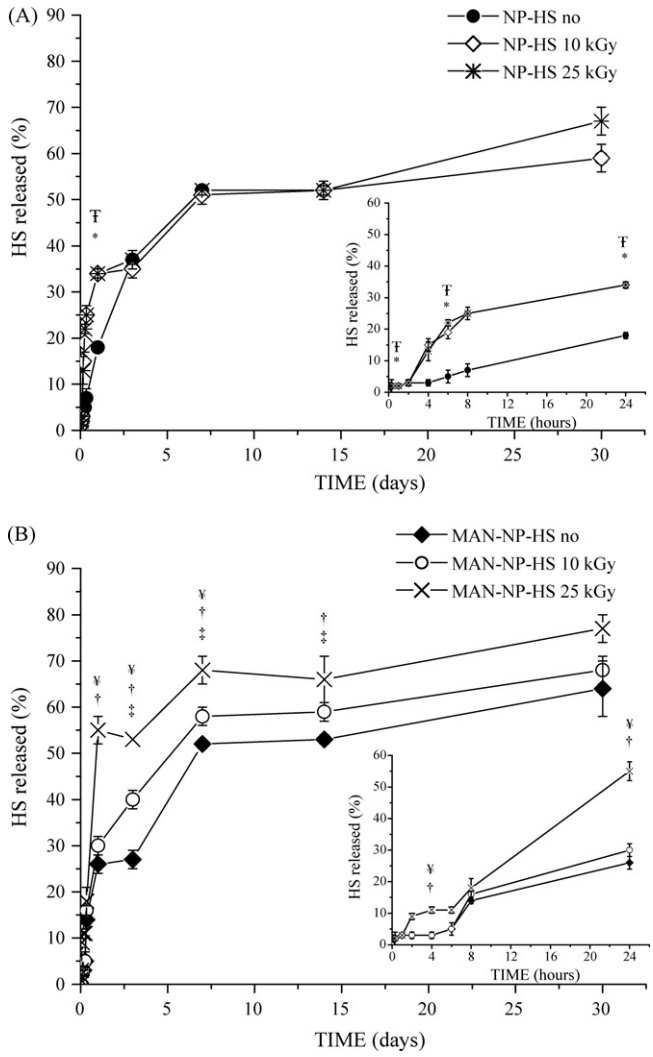

Fig. 4. Influence of the γ-irradiation on the release properties from HS containing nanoparticles. These graphs express in percentage the cumulative HS release from the formulations tested (BCA™ Protein Assay). (A) NP-HS no γ-irradiated (●), NP-HS γ-irradiated at 10 kGy (◊), NP-HS γ-irradiated at 25 kGy (Σ); B: MAN-NP-HS no γ-irradiated (♦), MAN-NP-HS γ-irradiated at 10 kGy (○) and MAN-NP-HS γ-irradiated at 25 kGy (×). Data express the mean ± S.D., $n = 3$. $^{*}p < 0.05$ for NP-HS no γ-irradiated vs. NP-HS γ-irradiated at 10 kGy (Mann–Whitney *U*-test). $^{\top}p < 0.05$ for NP-HS no γ-irradiated vs. NP-HS γ-irradiated at 25 kGy (Mann–Whitney *U*-test). $^{\ddagger}p < 0.05$ for MAN-NP-HS no γ-irradiated vs. MAN-NP-HS γ-irradiated at 10 kGy (Mann–Whitney *U*-test). $^{\dagger}p < 0.05$ for MAN-NP-HS no γ-irradiated vs. MAN-NP-HS γ-irradiated at 25 kGy (Mann–Whitney *U*-test). $^{¥}p < 0.05$ for MAN-NP-HS γ-irradiated at 10 kGy vs. MAN-NP-HS γ-irradiated at 25 kGy (Mann–Whitney *U*-test).

homogenous size distribution, high yield and effective antigen loading. The production of the mannosylated nanodevices took place by reaction of the mannose derivative with the copolymer before the formation of nanoparticles and by direct coating of the just formed carriers. This method, previously described (Salman et al., 2006), is based on the simple spontaneous reaction between the anhydride groups of the copolymer and the amino residues of the ligand to form amine bonds in an aqueous medium. As shown in Table 1, significant differences between both types of nanoparticle formulations were found for size and zeta potential, reflecting the presence of mannosamine on the surface of these carriers. These results are in agreement with other works in which it was also described an increase on both average size and electronegative charge for the mannosylated nanoparticles (Salman et al., 2006). By comparison of the physicochemical characteristics, irradiation did not seem to have a significant effect, since no apparent differences were observed between γ-irradiated and non-irradiated nanoparticles. These results show that no visible morphological changes (i.e. particle fusion) took place after sterilization. This fact has been also described by different authors working with different types of carriers and polymers, such as PLGA nanoparticles (Igartua et al., 2008; Martinez-Sancho et al., 2004), poly(butylcyanoacrylate) nanoparticles (Maksimenko et al., 2008), β-cyclodextrin nanocapsules (Memisoglu-Bilensoy and Hincal, 2006) and chitosan microparticles (Desai and Park, 2006).

The mannosamine content was alike for both empty and HS loaded mannosylated nanoparticles (about 30 μg/mg of nanoparticles). However, the polymer modifications slightly affected the HS loading ratio since conventional nanoparticles displayed a higher antigen loading than mannosylated ones. These observations agree well with previous data reported for mannose nanoparticles in which the payload was found to be lower comparing to the unconjugated ones (Jain et al., 2008; Salman et al., 2006). Furthermore, when comparing with HS loaded poly(ε-caprolactone) microparticles (Estevan et al., 2006), the entrapment into nanoparticles increased the HS loading. In fact, the antigenic complex was efficiently entrapped into poly(anhydride) nanoparticles with encapsulation efficiencies between 65% and 69%. Again, the sterilization process did not affect the antigen loading, as no significant differences were observed between irradiated and non-irradiated nanoparticles ($p > 0.05$). Furthermore, SDS-PAGE and immunoblotting demonstrated that there was no apparent modifications due to the γ-irradiation doses tested respectively on the antigen integrity and antigenicity. These results are in agreement with previous works reporting both the maintenance of the antigen loading and the absence of degradation of the antigens exposed to γ-irradiation (Igartua et al., 2008).

The following step was to study the presence and integrity of the mannosamine coating layer on the mannosylated nanoparticles. The results clearly demonstrated that Con A lectin was able to

Table 3
Pearson's correlation matrix of the cumulative HS release from the nanoparticles.

	NP-HS NO γ-irradiated	NP-HS 10 kGy	NP-HS 25 kGy	MAN-NP-HS NO γ-irradiated	MAN-NP-HS 10 kGy	MAN-NP-HS 25 kGy
NP-HS NO γ-irradiated	1					
NP-HS 10 kGy	0.946**	1				
NP-HS 25 kGy	0.946**	0.995**	1			
MAN-NP-HS NO γ-irradiated	0.981**	0.960**	0.967**	1		
MAN-NP-HS 10 kGy	0.990**	0.969**	0.967**	0.993**	1	
MAN-NP-HS 25 kGy	0.956**	0.972**	0.965**	0.966**	0.979**	1

NP-HS NO γ-irradiated: HS loaded conventional nanoparticles no γ-irradiated, $n = 13$. NP-HS 10 kGy: HS loaded conventional nanoparticles γ-irradiated at 10 kGy, $n = 13$. NP-HS 25 kGy: HS loaded conventional nanoparticles γ-irradiated at 25 kGy, $n = 13$. MAN-NP-HS NO γ-irradiated: HS loaded mannosylated nanoparticles no γ-irradiated, $n = 13$. MAN-NP-HS 10 kGy: HS loaded mannosylated nanoparticles γ-irradiated at 10 kGy, $n = 13$. MAN-NP-HS 25 kGy: HS loaded mannosylated nanoparticles γ-irradiated at 25 kGy, $n = 13$.

** Correlation is significant at the 0.01 level (2-tailed).

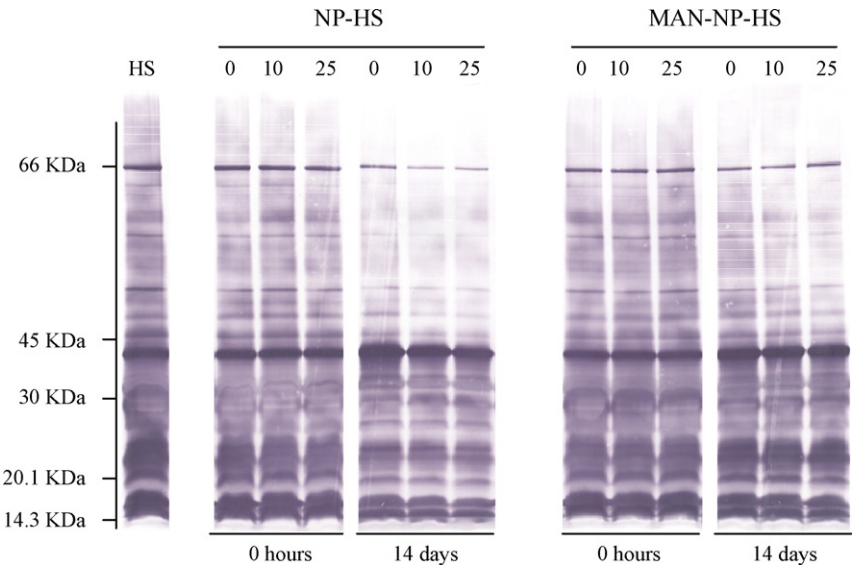

Fig. 5. Western blot against a pool of sera from *B. ovis* experimentally infected rabbits of the HS antigenic extract entrapped into nanoparticles, during the kinetic release. Lanes: HS: 40 μg free hot saline antigenic extract; NP-HS: HS loaded conventional nanoparticles; MAN-NP-HS: HS loaded mannosylated nanoparticles. (0) Non-γ-irradiated; (10) γ-irradiation dose of 10 kGy and (25) γ-irradiation dose of 25 kGy.

strongly interact with mannosylated nanoparticles or γ-irradiated nanoparticles at 10 kGy. However mannosylated nanoparticles previously exposed to a γ-irradiation dose of 25 kGy exhibited a weaker reactivity (see Fig. 2). This different agglutination behaviour may be related to a radiolysis phenomenon that may increase cross-linking and promote a chain cleavage effect (Calis et al., 2002; Faisant et al., 2002; Masson et al., 1997). Previous studies reported that oxidation by γ-irradiation may negatively affect the stability of peptide bonds (Carrascosa et al., 2003; Rothen-Weinhold et al., 1999), likewise the amide bonds between the polymer and mannosamine moieties were probably affected which resulted in the partial loss of mannose activity.

Besides the target ligand, radiosterilization may also induce polymer changes. To evaluate the effect of γ-irradiation on the antigen release from vaccine formulations it was performed an *in vitro* study simulating the physiological conditions during 30 days, with the non-irradiated nanoparticles as reference. The HS release profile from nanoparticles was biphasic and characterized by a 24 h burst effect followed by a continuous release. The second part of the kinetic profile was quite similar when compared the accumulated HS released. Similar results were obtained in analogous studies (Carrascosa et al., 2003) where the γ-sterilization lead to an increased initial release, but did not affect the release rate during the subsequent phase. Interestingly, the Pearson's correlation matrix of the cumulative antigen released from the nanoparticles (Table 3) revealed that, independently of the type of poly(anhydride) nanoparticle or the irradiation intensity, all the release patterns followed a similar tendency.

For conventional nanoparticles, the sterilization process appeared to modify the antigenic release behaviour during the first 24 h ($p < 0.05$), however after the 30 days all the formulations released the same antigenic amount ($p > 0.05$). On the other hand, mannosylation induced an increase of the HS released during the first 24 h. Interestingly, the irradiation dose of 25 kGy caused a significant burst effect two times higher than the release observed for other vaccine formulations. This observation agrees well with the susceptibility to high irradiation doses already demonstrated by the concanavalin A agglutination assay. In addition, it is known that poly(anhydride) devices are surface eroding under a size of approximately 100 μm (Gopferich and Tessmar, 2002). This eroded zone is

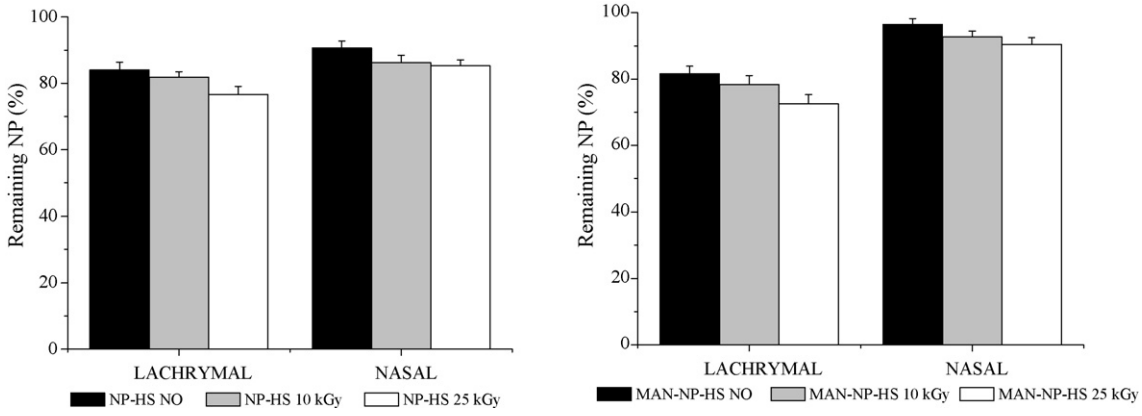

Fig. 6. Nanoparticle stability at 2 h post-incubation, expressed in percentage, after incubation in lachrymal fluid and nasal secretions. NP-HS: HS loaded conventional nanoparticles; MAN-NP-HS: HS loaded mannosylated nanoparticles (data expressed as mean ± S.D., at least $n = 3$).

a key parameter influencing the drug release from poly(anhydride) devices. Since the presence of mannosamine would increase the porosity and the tortuosity of the resulting nanoparticles, the release of HS would be facilitate. On the other hand, the antigen release rate also increased with higher γ-irradiation doses. This observation is in agreement with Desai and coworkers (Desai and Park, 2006), who reported that the release rate from γ-irradiated chitosan microspheres was significantly faster. In the same way, it was also reported the negative influence of the 25 kGy dose on the release of bupivacaine from PLGA nanoparticles (Montanari et al., 2002).

The HS released from non-irradiated and γ-irradiated nanoparticles after 14 days maintained its protein profile, as well as its integrity and antigenicity. Among them, Omp31 is of a particular interest in *B. ovis* infection, since it may be the immunodominant antigen in the antibody responses of naturally and experimentally infected rams (Kittelberger et al., 1995). In this context, HS containing nanoparticles, submitted to both γ-irradiation doses, can be able to, at least along 14 days, ensure the release of the antigenic extract from a sustained delivery manner and maintain the *in vitro* biological activity.

Finally, it was studied the stability of the different nanoparticle formulations in lachrymal and nasal ovine fluids directly obtained from rams. After 2 h of incubation in these fluids, the remaining nanoparticles were of about 95–75%. However, the HS released at this time did not reach more than 10% (Fig. 4). Thus, considering the release study, although nanoparticles were already initiating the degradation phenomenon, smaller polymer–HS micelle complexes could be delivering antigen.

The slightly lower stability in the lachrymal than in the nasal fluids would be probably due to higher water accessibility. Nasal secretions present higher viscosity and acidity, which hindered water access to the surface of the nanoparticles and further hydrolysis of the polymer or surface erosion of the nanoparticles. In agreement with the nanoparticles kinetic release, increased γ-sterilization doses accelerated the degradation of the nanoparticles in aqueous media. On the other hand, mannosylation increased the stability in nasal fluid. A similar increase of the stability of these poly(anhydride) nanoparticles has been reported by cross-linkage with 1,3-diaminopropane or coating with ligands (i.e. BSA) (Arbos et al., 2003).

The pharmacopoeial sterility biological tests were applied for samples exposed to doses under 25 kGy without any evidence of microbial growth for the nanoparticles γ-irradiated at 10 kGy. In what concerns to the non-irradiated nanoparticles, there was only evidence of aerobic bacterial growth. Furthermore, the sterility of the samples γ-irradiated at 10 kGy and 25 kGy was maintained for at least 2 years.

5. Conclusions

In order to deliver vaccine antigens to mucosal surfaces, conventional and mannosylated poly(anhydride) nanoparticles loaded with an antigenic complex from *B. ovis* were designed. This is the first report describing the successful entrapment of these bacterial antigens in both conventional and mannosylated nanoparticles. Furthermore, the physicochemical properties of these nanoparticles formulations, as well as the integrity and antigenicity of the antigenic complex, were not affected by sterilization with γ-irradiation. Nevertheless, in spite of all the release patterns followed a similar tendency, the use of 25 kGy dose appeared to negatively influence the HS release. In any case, it is necessary to establish the real protective value of these vaccine systems with additional research performed in natural hosts.

Acknowledgements

The authors are grateful to Prof. Dr. Rafael Jordana from the University of Navarra for the SEM analysis. This work was supported by "Fundação para a Ciência e a Tecnologia" (SFRH/BD/41703/2007) in Portugal, "Asociación de Amigos de la Universidad de Navarra", "Fundación Caja Navarra: Tú eliges, tú decides" (Nanotecnología y Medicamentos, n°10828) and grants from the "Ministerio de Ciencia y Inovación" (AGL2004-07088-C03-01/GAN and -02/GAN)" in Spain.

References

Almeida, A.J., Alpar, H.O., 1996. Nasal delivery of vaccines. J. Drug Target. 3, 455–467.
Araya, L.N., Winter, A.J., 1990. Comparative protection of mice against virulent and attenuated strains of *Brucella abortus* by passive transfer of immune T cells or serum. Infect. Immun. 58, 254–256.
Arbos, P., Campanero, M.A., Arangoa, M.A., Renedo, M.J., Irache, J.M., 2003. Influence of the surface characteristics of PVM/MA nanoparticles on their bioadhesive properties. J. Control. Release 89, 19–30.
Arbos, P., Wirth, M., Arangoa, M.A., Gabor, F., Irache, J.M., 2002. Gantrez AN as a new polymer for the preparation of ligand–nanoparticle conjugates. J. Control. Release 83, 321–330.
Benson, J.R., Hare, P.E., 1975. O-phthalaldehyde: fluorogenic detection of primary amines in the picomole range. Comparison with fluorescamine and ninhydrin. Proc. Natl. Acad. Sci. U.S.A. 72, 619–622.
Blasco, J.M., 1997. A review of the use of *B. melitensis* Rev 1 vaccine in adult sheep and goats. Prev. Vet. Med. 31, 275–283.
Blasco, J.M., Diaz, R., 1993. *Brucella melitensis* Rev-1 vaccine as a cause of human brucellosis. Lancet 342, 805.
Blasco, J.M., Gamazo, C., Winter, A.J., Jimenez de Bagues, M.P., Marin, C., Barberan, M., Moriyon, I., Alonso-Urmeneta, B., Diaz, R., 1993. Evaluation of whole cell and subcellular vaccines against *Brucella ovis* in rams. Vet. Immunol. Immunopathol. 37, 257–270.
Boschiroli, M.L., Foulongne, V., O'Callaghan, D., 2001. Brucellosis: a worldwide zoonosis. Curr. Opin. Microbiol. 4, 58–64.
Calis, S., Bozdag, S., Kas, H.S., Tuncay, M., Hincal, A.A., 2002. Influence of irradiation sterilization on poly(lactide-co-glycolide) microspheres containing anti-inflammatory drugs. Farmaco 57, 55–62.
Carrascosa, C., Espejo, L., Torrado, S., Torrado, J.J., 2003. Effect of gamma-sterilization process on PLGA microspheres loaded with insulin-like growth factor-I (IGF-I). J. Biomater. Appl. 18, 95–108.
Cutler, S.J., Whatmore, A.M., Commander, N.J., 2005. Brucellosis—new aspects of an old disease. J. Appl. Microbiol. 98, 1270–1281.
Desai, K.G., Park, H.J., 2006. Study of gamma-irradiation effects on chitosan microparticles. Drug Deliv. 13, 39–50.
Engering, A.J., Cella, M., Fluitsma, D., Brockhaus, M., Hoefsmit, E.C., Lanzavecchia, A., Pieters, J., 1997. The mannose receptor functions as a high capacity and broad specificity antigen receptor in human dendritic cells. Eur. J. Immunol. 27, 2417–2425.
Estevan, M., Gamazo, C., Grillo, M.J., Del Barrio, G.G., Blasco, J.M., Irache, J.M., 2006. Experiments on a sub-unit vaccine encapsulated in microparticles and its efficacy against *Brucella melitensis* in mice. Vaccine 24, 4179–4187.
European Pharmacopoeia 6th ed, 2007. Council of Europe, Strasbourg Cedex, France.
Faisant, N., Siepmann, J., Oury, P., Laffineur, V., Bruna, E., Haffner, J., Benoit, J., 2002. The effect of gamma-irradiation on drug release from bioerodible microparticles: a quantitative treatment. Int. J. Pharm. 242, 281–284.
Figdor, C.G., van Kooyk, Y., Adema, G.J., 2002. C-type lectin receptors on dendritic cells and Langerhans cells. Nat. Rev. Immunol. 2, 77–84.
Gamazo, C., Winter, A.J., Moriyon, I., Riezu-Boj, J.I., Blasco, J.M., Diaz, R., 1989. Comparative analyses of proteins extracted by hot saline or released spontaneously into outer membrane blebs from field strains of *Brucella ovis* and *Brucella melitensis*. Infect. Immun. 57, 1419–1426.
Gomez, S., Gamazo, C., Roman, B.S., Ferrer, M., Sanz, M.L., Irache, J.M., 2007. Gantrez AN nanoparticles as an adjuvant for oral immunotherapy with allergens. Vaccine 25, 5263–5271.
Gopferich, A., Tessmar, J., 2002. Polyanhydride degradation and erosion. Adv. Drug Deliv. Rev. 54, 911–931.
Greenfield, R.A., Drevets, D.A., Machado, L.J., Voskuhl, G.W., Cornea, P., Bronze, M.S., 2002. Bacterial pathogens as biological weapons and agents of bioterrorism. Am. J. Med. Sci. 323, 299–315.
Igartua, M., Hernandez, R.M., Rosas, J.E., Patarroyo, M.E., Pedraz, J.L., 2008. Gamma-irradiation effects on biopharmaceutical properties of PLGA microspheres loaded with SPf66 synthetic vaccine. Eur. J. Pharm. Biopharm. 69, 519–526.
Irache, J.M., Salman, H.H., Gamazo, C., Espuelas, S., 2008. Mannose-targeted systems for the delivery of therapeutics. Expert Opin. Drug Deliv. 5, 703–724.
Jain, S., Vyas, S.P., 2006. Mannosylated niosomes as adjuvant-carrier system for oral mucosal immunization. J. Liposome Res. 16, 331–345.
Jain, S.K., Gupta, Y., Jain, A., Saxena, A.R., Khare, P., Jain, A., 2008. Mannosylated gelatin nanoparticles bearing an anti-HIV drug didanosine for site-specific delivery. Nanomedicine 4, 41–48.

Jimenez de Bagues, M.P., Barberan, M., Marin, C.M., Blasco, J.M., 1995. The *Brucella abortus* RB51 vaccine does not confer protection against *Brucella ovis* in rams. Vaccine 13, 301–304.

Keler, T., Ramakrishna, V., Fanger, M.W., 2004. Mannose receptor-targeted vaccines. Expert Opin. Biol. Ther. 4, 1953–1962.

Kittelberger, R., Hilbink, F., Hansen, M.F., Ross, G.P., de Lisle, G.W., Cloeckaert, A., de Bruyn, J., 1995. Identification and characterization of immunodominant antigens during the course of infection with *Brucella ovis*. J. Vet. Diagn. Invest. 7, 210–218.

Lambert, G., Fattal, E., Pinto-Alphandary, H., Gulik, A., Couvreur, P., 2000. Poly-isobutylcyanoacrylate nanocapsules containing an aqueous core as a novel colloidal carrier for the delivery of oligonucleotides. Pharm. Res. 17, 707–714.

Maksimenko, O., Pavlov, E., Toushov, E., Molin, A., Stukalov, Y., Prudskova, T., Feldman, V., Kreuter, J., Gelperina, S., 2008. Radiation sterilisation of doxorubicin bound to poly(butyl cyanoacrylate) nanoparticles. Int. J. Pharm. 356, 325–332.

Martinez-Sancho, C., Herrero-Vanrell, R., Negro, S., 2004. Study of gamma-irradiation effects on aciclovir poly(D, L-lactic-co-glycolic) acid microspheres for intravitreal administration. J. Control. Release 99, 41–52.

Masson, V., Maurin, F., Fessi, H., Devissaguet, J.P., 1997. Influence of sterilization processes on poly(epsilon-caprolactone) nanospheres. Biomaterials 18, 327–335.

Memisoglu-Bilensoy, E., Hincal, A.A., 2006. Sterile, injectable cyclodextrin nanoparticles: effects of gamma irradiation and autoclaving. Int. J. Pharm. 311, 203–208.

Montanari, L., Cilurzo, F., Conti, B., Genta, I., Groppo, A., Valvo, L., Faucitano, A., Buttafava, A., 2002. Gamma irradiation effects and EPR investigation on poly(lactide-co-glycolide) microspheres containing bupivacaine. Farmaco 57, 427–433.

Moriyon, I., Grillo, M.J., Monreal, D., Gonzalez, D., Marin, C., Lopez-Goni, I., Mainar-Jaime, R.C., Moreno, E., Blasco, J.M., 2004. Rough vaccines in animal brucellosis: structural and genetic basis and present status. Vet. Res. 35, 1–38.

Motwani, S.K., Chopra, S., Talegaonkar, S., Kohli, K., Ahmad, F.J., Khar, R.K., 2008. Chitosan-sodium alginate nanoparticles as submicroscopic reservoirs for ocular delivery: formulation, optimisation and in vitro characterisation. Eur. J. Pharm. Biopharm. 68, 513–525.

Munoz, P.M., Estevan, M., Marin, C.M., Jesus De Miguel, M., Jesus Grillo, M., Barberan, M., Irache, J.M., Blasco, J.M., Gamazo, C., 2006. Brucella outer membrane complex-loaded microparticles as a vaccine against *Brucella ovis* in rams. Vaccine 24, 1897–1905.

Murillo, M., Grillo, M.J., Rene, J., Marin, C.M., Barberan, M., Goni, M.M., Blasco, J.M., Irache, J.M., Gamazo, C., 2001. A *Brucella ovis* antigenic complex bearing poly-epsilon-caprolactone microparticles confer protection against experimental brucellosis in mice. Vaccine 19, 4099–4106.

Oliveira, S.C., Splitter, G.A., 1995. CD8+ type 1 CD44hi CD45 RBlo T lymphocytes control intracellular *Brucella abortus* infection as demonstrated in major histocompatibility complex class I- and class II-deficient mice. Eur. J. Immunol. 25, 2551–2557.

Osborn, M.J., 1963. Studies on the gram-negative cell wall. I. Evidence for the role of 2-keto-3-deoxyoctonate in the lipopolysaccharide of *Salmonella typhimurium*. Proc. Natl. Acad. Sci. U.S.A. 50, 499–506.

Ramakrishna, V., Vasilakos, J.P., Tario Jr., J.D., Berger, M.A., Wallace, P.K., Keler, T., 2007. Toll-like receptor activation enhances cell-mediated immunity induced by an antibody vaccine targeting human dendritic cells. J. Transl. Med. 5, 5.

Rothen-Weinhold, A., Besseghir, K., Vuaridel, E., Sublet, E., Oudry, N., Gurny, R., 1999. Stability studies of a somatostatin analogue in biodegradable implants. Int. J. Pharm. 178, 213–221.

Salman, H.H., Gamazo, C., Campanero, M.A., Irache, J.M., 2006. Bioadhesive mannosylated nanoparticles for oral drug delivery. J. Nanosci. Nanotechnol. 6, 3203–3209.

Salman, H.H., Gomez, S., Gamazo, C., Costa Martins, R., Zabaleta, V., Irache, J.M., 2008. Micro-organism-like nanoparticles for oral antigen delivery. J. Drug Del. Sci. Technol. 18, 31–39.

Schurig, G.G., Roop 2nd, R.M., Bagchi, T., Boyle, S., Buhrman, D., Sriranganathan, N., 1991. Biological properties of RB51: a stable rough strain of *Brucella abortus*. Vet. Microbiol. 28, 171–188.

Schurig, G.G., Sriranganathan, N., Corbel, M.J., 2002. Brucellosis vaccines: past, present and future. Vet. Microbiol. 90, 479–496.

Smith, P.K., Krohn, R.I., Hermanson, G.T., Mallia, A.K., Gartner, F.H., Provenzano, M.D., Fujimoto, E.K., Goeke, N.M., Olson, B.J., Klenk, D.C., 1985. Measurement of protein using bicinchoninic acid. Anal. Biochem. 150, 76–85.

Whatmore, A.M., Dawson, C.E., Groussaud, P., Koylass, M.S., King, A.C., Shankster, S.J., Sohn, A.H., Probert, W.S., McDonald, W.L., 2008. Marine mammal Brucella genotype associated with zoonotic infection. Emerg. Infect. Dis. 14, 517–518.

Young, E.J., 1995. An overview of human brucellosis. Clin. Infect. Dis. 21, 283–289 (quiz 290).